HHS Public Access

Author manuscript

Immunity. Author manuscript; available in PMC 2016 April 21.

Published in final edited form as:

Immunity. 2015 April 21; 42(4): 679–691. doi:10.1016/j.immuni.2015.03.013.

Methyl-CpG binding protein 2 regulates microglia and macrophage gene expression in response to inflammatory stimuli

James C. Cronk[1,2,3,4,*], **Noël C. Derecki**[1,2,3,*], **Emily Ji**[1,2], **Yang Xu**[8], **Aaron E. Lampano**[8], **Igor Smirnov**[1,2], **Wendy Baker**[1,2], **Geoffrey T. Norris**[1,2,3], **Ioana Marin**[1,2,3], **Nathan Coddington**[1,2], **Yochai Wolf**[9], **Stephen D. Turner**[6], **Alan Aderem**[10], **Alexander L. Klibanov**[5,7], **Tajie H. Harris**[1,2,3], **Steffen Jung**[9], **Vladimir Litvak**[8,#], and **Jonathan Kipnis**[1,2,3,4,#]

[1]Center for Brain Immunology and Glia, School of Engineering and Applied Science, University of Virginia, Charlottesville, VA 22908, USA

[2]Department of Neuroscience, School of Engineering and Applied Science, University of Virginia, Charlottesville, VA 22908, USA

[3]Graduate, Program in Neuroscience, School of Engineering and Applied Science, University of Virginia, Charlottesville, VA 22908, USA

[4]Medical Scientist Training Program, School of Engineering and Applied Science, University of Virginia, Charlottesville, VA 22908, USA

[5]Cardiovascular, Research Center, Cardiovascular Division, Department of Internal Medicine, School of Engineering and Applied Science, University of Virginia, Charlottesville, VA 22908, USA

Correspondence should be addressed to V.L. (vladimir.litvak@umassmed.edu) or J.K. (kipnis@virginia.edu). Tel: 434-982-3858, Fax: 434-982-4380.

*Equal contribution

#Equally contributing senior authors

Author contributions

J.C. Cronk and N.C. Derecki designed the experiments, performed the experiments, analyzed the data, and wrote the manuscript.
E. Ji assisted with flow cytometry and immunohistochemistry experiments.
Y. Xu analyzed RNA-Seq data and performed *in vitro* experiments.
A. Lampano performed *in vitro* experiments.
I. Smirnov participated in all experiments with experimental animals.
W. Baker assisted with maintenance and genotyping of experimental animals.
G.T. Norris performed the microglia Sholl analysis.
I. Marin assisted with intestinal preparations.
N. Coddington assisted with *in vitro* experiments.
A. Aderem provided ChIP-Seq data.
Y. Wolf and S. Jung generated and provided the transgenic mice (*Cx3cr1*^{creER}).
A. Klibanov provided liposomes.
T. Harris assisted with the intravital experiments.
V. Litvak designed the experiments, analyzed data, and wrote the manuscript.
J. Kipnis conceived and led the project, designed the experiments and wrote the manuscript.

[6]Department of Public Health Sciences, School of Medicine, School of Engineering and Applied Science, University of Virginia, Charlottesville, VA 22908, USA

[7]Department of Biomedical, Engineering, School of Engineering and Applied Science, University of Virginia, Charlottesville, VA 22908, USA

[8]Department of Microbiology and Physiological Systems, University of Massachusetts Medical School, Worcester, MA 01655, USA

[9]Department of Immunology, Weizmann Institute of Science, Rehovot Israel 76100

[10]Seattle Biomedical Research Institute, Seattle, WA 98109, USA

Summary

Mutations in *MECP2*, encoding the epigenetic regulator methyl-CpG-binding protein 2, are the predominant cause of Rett syndrome, a disease characterized by both neurological symptoms and systemic abnormalities. Microglial dysfunction is thought to contribute to disease pathogenesis, and here we found microglia become activated and subsequently lost with disease progression in Mecp2-null mice. Mecp2 was found to be expressed in peripheral macrophage and monocyte populations, several of which also became depleted in Mecp2-null mice. RNA-seq revealed increased expression of glucocorticoid- and hypoxia-induced transcripts in Mecp2-null microglia and peritoneal macrophages. Furthermore, Mecp2 was found to regulate inflammatory gene transcription in response to TNF stimulation. Postnatal re-expression of Mecp2 using $Cx3cr1^{creER}$ increased the lifespan of otherwise Mecp2-null mice. These data suggest Mecp2 regulates microglia and macrophage responsiveness to environmental stimuli to promote homeostasis. Dysfunction of tissue-resident macrophages may contribute to the systemic pathologies observed in Rett syndrome.

Introduction

Rett syndrome, caused primarily by mutations in methyl-CpG binding protein 2 (MeCP2) (Amir et al., 1999), features prominent neurologic sequelae (Chahrour and Zoghbi, 2007); accordingly, efforts to understand the function of MeCP2 have been focused largely on its role in neurons (Chahrour and Zoghbi, 2007). Recent reports have found expression and roles for Mecp2 in astrocytes (Ballas et al., 2009; Lioy et al.; Yasui et al., 2013), oligodendrocytes (Nguyen et al., 2013), and microglia (Derecki et al., 2012; Maezawa and Jin, 2010). In addition, Mecp2 is expressed in many tissues (Shahbazian et al., 2002). Thus, mutations in MeCP2 likely affect multiple organ systems and cell types, which is indeed reflected in the complexity of symptoms associated with Rett syndrome (Chahrour and Zoghbi, 2007; Dunn and MacLeod, 2001). While neurological symptoms are prominent, most girls with Rett syndrome also suffer from somatic impairments, including stunted growth, osteopenia, scoliosis, and digestive difficulties (Chahrour and Zoghbi, 2007; Dunn and MacLeod, 2001).

Many tissue-resident macrophages, including microglia, originate during embryonic hematopoiesis, beginning in the yolk sac and moving to the fetal liver. These precursor cells disseminate throughout tissues during embryogenesis, engraft within nearly every organ

system, and form self-renewing populations (Ginhoux et al., 2010; Hashimoto et al., 2013; Kierdorf et al., 2013; Schulz et al., 2012; Yona et al., 2013). Other populations of tissue-resident macrophages, such as intestinal lamina propria intestinal macrophages, are constantly replenished by circulating monocytes (Bain et al., 2013; Varol et al., 2009). The functional roles of tissue-resident macrophages vary greatly, and are dependent upon location and context (Davies et al., 2013). However, all tissue-resident macrophages appear to be unified by their role as provisioners of homeostatic maintenance (Davies et al., 2013). Further, monocyte-derived inflammatory non-resident macrophages are critical for effective response to infection and injury. In this context, these cells rely on a carefully balanced network of skewing paradigms, which direct macrophage function including the initiation and resolution of inflammation, clearance of debris and pathogens, and assistance in the healing process (Sica and Mantovani, 2012). Notably, mice lacking macrophage colony stimulating factor 1 receptor (CSF-1R) are deficient in all macrophages and are characterized by multiple organ failures and shortened lifespan (Dai et al., 2002), emphasizing the critical importance of macrophages in support of bodily tissues.

Our previous work demonstrated that engraftment of wild type monocytes into the brains of Mecp2-null mice (through bone marrow transplantation) extends lifespan by several months and improves neurologic and behavioral outcomes (Derecki et al., 2012). In addition, phagocytosis of apoptotic cells *in vitro* is impaired in Mecp2-null microglia. Although brain engraftment by monocytes with bone marrow transplant is crucial for significant lifespan extension in Mecp2-null mice (Derecki et al., 2012), we did not explore the possibility that Mecp2 might be important for the normal function of other mononuclear phagocytes.

Here we demonstrated that numerous populations of macrophages and monocytes expressed Mecp2, and that Mecp2-null mice become deficient in several macrophage populations, including microglia. We next showed that postnatal re-expression of *Mecp2* under a *Cx3cr1*-inducible promoter resulted in a lifespan increase in otherwise Mecp2-null mice. In order to elucidate mechanisms behind the macrophage defects in the context of Mecp2-deficiency, we demonstrated by RNA-Seq that acutely isolated Mecp2-null microglia and peritoneal macrophages displayed changes in specific signaling pathways, suggesting that Mecp2 is an important regulator of microglia/macrophage gene expression. Further *in vivo* and *in vitro* validation studies confirmed that Mecp2 is important for proper transcriptional regulation of multiple gene expression programs in macrophages. Overall, these results demonstrated that Mecp2 is an important epigenetic regulator of macrophage response to stimuli and stressors.

Results

Microglia become activated and subsequently depleted with disease progression in Mecp2-null mice

Our previous data (Derecki et al., 2012) showing a role for microglia in disease pathogenesis of Mecp2-deficient mice led us to study in greater detail the role of Mecp2 in microglia and developmentally related peripheral tissue-resident macrophages. Wild type microglia were found to express Mecp2, as examined by intracellular flow cytometric labeling (Figure 1A) or by *in situ* immunofluorescence (Figure 1B). This is in line with previously reported results (Maezawa and Jin, 2010).

We next investigated how loss of Mecp2 affects microglia *in vivo*. Using a thinned-skull technique, we performed intravital two-photon imaging on pre- and late-phenotypic Mecp2-null and wild type mice. We observed that pre-phenotypic Mecp2-null microglia had significantly smaller somas (similar to Mecp2-null neurons and astrocytes), while late-phenotypic Mecp2-null microglia soma were larger in size as compared to wild type (Figure 1C and 1D; Movies S1 and S2), suggestive of microglia activation (Kozlowski and Weimer, 2012). In addition, *in situ* Sholl analysis demonstrated that while pre-phenotypic Mecp2-null microglia were not different from wild type, microglia from late-phenotypic mice displayed significantly reduced process complexity in three examined brain areas (hippocampus, neocortex and cerebellum; Figure 1E). Together, the findings of increased soma size and decreased process complexity suggested that Mecp2-null microglia became activated with disease progression. Indeed, qRT-PCR of acutely isolated Mecp2-null microglia from pre- and late-phenotypic mice showed increased *Tnf* mRNA encoding the pro-inflammatory cytokine tumor necrosis factor (TNF) (Figure 1F) while *Tgfb1* transcription, required for microglia maintenance (Butovsky et al., 2014), was decreased in late-phenotypic microglia (Figure 1G).

We next examined Mecp2-null microglia by flow cytometry, which revealed a progressive loss of microglia in Mecp2-null mice from pre- to late-phenotypic stage (Figure 1H and 1I). Loss of microglia was found throughout the brain (Figure 1J). The loss was also observed in brains of late-phenotypic Mecp2-null mice by immunohistochemistry (Figure S1A and S1B). Further, immunohistochemical staining for Iba1, a microglial marker, and for cleaved caspase 3 (CC3), a marker of apoptotic cells, revealed sporadic $CC3^{+}$ microglia in late-phenotypic Mecp2-null brains (Figure S1C). In sum, these data suggest that in the context of Mecp2-deficiency, microglia become activated and are lost with disease progression.

Meningeal macrophages are lost with disease progression in Mecp2-null mice

When analyzing microglia by intravital two-photon microscopy, we also observed significant morphologic disruption of $Cx3cr1^{GFP/+}$ meningeal macrophages *in vivo* in late-phenotypic Mecp2-null mice suggestive of reactive phenotype (Figure 2A). To assess meningeal macrophages in further detail, we performed immunofluorescent labeling of meninges from pre-, mid-, and late-phenotypic Mecp2-null mice using antibodies against CD163 and F4/80. A progressive loss of macrophages at the late-phenotypic state was evident in Mecp2-null mice (Figure 2B and 2C).

Perivascular macrophages in the meninges are $F4/80^{+}CD163^{+}$, while a separate meningeal macrophage population is $F4/80^{+}CD163^{-}$ (Davies et al., 2013). When we analyzed these populations separately, we found that perivascular macrophages ($F4/80^{+}CD163^{+}$) were progressively lost in Mecp2-null mice (Figure 2D), while non-perivascular meningeal macrophages ($F4/80^{+}CD163^{-}$) were not significantly depleted (Figure 2E).

Peripheral monocytes and macrophages express Mecp2, and some are lost in Mecp2-null mice

Given the phenotype of meningeal macrophages and microglia, we decided to expand our analysis to additional populations of peripheral macrophages. Many tissue-resident

macrophages, including microglia, originate from similar progenitor pools during embryogenesis (Ginhoux et al., 2010; Hashimoto et al., 2013; Kierdorf et al., 2013; Schulz et al., 2012; Yona et al., 2013), and might therefore share pathologies in the context of Mecp2-deficiency. We found that all tested tissue-resident macrophages expressed Mecp2 (Figure 3A and 3B). In addition, Ly6c^{lo} monocytes, which represent a longer-lived resident population in the blood (Yona et al., 2013) also expressed Mecp2 (Figure 3B). In contrast, Ly6c^{hi}CCR2^{+} monocytes and neutrophils expressed low or undetectable amounts of Mecp2 (Figure 3C).

As expected, based on the microglia and meningeal macrophage results described above, we found reductions of other peripheral macrophage populations in Mecp2-null mice. Unlike microglia, CD64^{+}F4/80^{+}CD11b^{+} macrophages from the small intestine were reduced in both pre- and late-phenotypic Mecp2-null mice (Figure 3D and 3E). Circulating Ly6c^{lo} monocytes were also reduced in number in both pre- and late-phenotypic Mecp2-null mice (Figure 3F and 3G).

Since both CD64^{+}F4/80^{+}CD11b^{+} intestinal macrophages and Ly6c^{lo} monocytes share their derivation from Ly6c^{hi} monocytes (Bain et al., 2013; Varol et al., 2009; Yona et al., 2013), it is possible that the reductions seen in these populations even in pre-phenotypic Mecp2-null mice may reflect their common origin. To this end, we tested whether Ly6c^{hi} monocytes from bone marrow were impaired in their ability to differentiate and/or proliferate as macrophages in response to MCSF *in vitro*. We found that Mecp2-null Ly6c^{hi} monocytes differentiated into macrophages with similar kinetics to wild type and produced similar numbers of macrophages per monocyte, making it an unlikely possibility that Mecp2 is directly necessary for Ly6c^{hi} monocyte differentiation or macrophage proliferation in the absence of other factors (Figure S2).

Although Mecp2 did not affect differentiation or proliferation *in vitro*, we hypothesized that Mecp2 might play a role in monocyte/macrophage responses within the context of the full disease caused by whole-animal Mecp2-deficiency. To test this possibility, we depleted monocytes and macrophages using IV clodronate liposomes in wild type and Mecp2-null littermates (mid-phenotypic, ~6 weeks to allow for immune system maturation but prior to the peak of disease), and measured the repopulation of resident monocytes. DiI liposomes were injected IV two days after clodronate liposome injection, similar to published protocols (Sunderkotter et al., 2004). Ly6c^{hi} monocytes released from the bone marrow become DiI labeled and can be tracked in their differentiation to Ly6c^{lo} monocytes. On day 5 post-clodronate injection (day 3 post DiI), wild type and Mecp2-null mice had, as expected, begun to reconstitute their circulating monocyte populations, with a non-significant trend towards fewer total monocytes (CD115^{+}CD11b^{+}) in Mecp2-null mice (Figure 3H and 3I). However, when total monocytes were examined, Mecp2-null mice had significantly fewer resident Ly6c^{lo} monocytes as compared to wild type (Figure 3J). In addition, when only DiI^{+} monocytes were examined (representing only the circulating monocytes present on day 2 post-clodronate injection), DiI^{+} monocytes in wild type mice had almost completely differentiated into Ly6c^{lo} resident monocytes, while Mecp2-null mice displayed a deficit in Ly6c^{lo} monocyte differentiation (Figure 3K). The fact that some populations were deficient in the pre-phenotypic state (resident monocytes and intestinal macrophages), but others were

lost progressively (microglia and meningeal perivascular macrophages) led us to hypothesize that Mecp2 is likely playing a complex role in macrophage biology which is not limited to macrophage survival and/or death. Of note, we did not observe any difference in $CD163^{-}F4/80^{+}$ meningeal macrophages (Figure 2E) or splenic red pulp macrophages (data not shown), which also express Mecp2 (Figure 3A and 3B), further suggesting that the role of Mecp2 in macrophages is complex or upstream of cell loss and/or death, since not all macrophage populations were equally affected by Mecp2-deficiency. In addition, our data regarding microglia suggested inflammatory activation (Figure 1C–G), implicating Mecp2-deficiency in processes beyond simple loss of microglia/macrophages. Overall, the data suggested a complex role for Mecp2 in macrophages, consistent with its previously described role in other cell types as an epigenetic regulator, affecting a multitude of genes (Guy et al., 2011).

Postnatal expression of Mecp2 via *Cx3cr1^{creER}* in otherwise Mecp2-deficient mice increases lifespan

Previously we showed that transplantation of Mecp2-null mice with wild type bone marrow increases lifespan, and that engraftment of microglia-like cells into the brain is important for this effect (Derecki et al., 2012). More recently *Cx3cr1^{creER}* mice have become available (Goldmann et al., 2013; Yona et al., 2013), and microglia are among a subset of macrophages with high expression of CX3CR1 during adulthood (Jung et al., 2000). Thus the *Cx3cr1^{creER}* mouse can be used to efficiently target microglia, in addition to other CX3CR1-expressing monocytes and macrophages. Therefore, we crossed *Cx3cr1^{creER}* mice with *Mecp2$^{Lox\text{-}stop}$* mice and their offspring (*Cx3cr1$^{creER/+}$Mecp2$^{Lox\text{-}stop/y}$*) were treated with tamoxifen (~9 weeks of age), when symptoms just started to appear. In line with our previous finding with bone marrow transplantation (Derecki et al., 2012), the lifespan of tamoxifen-treated *Cx3cr1$^{creER/+}$Mecp2$^{Lox\text{-}stop/y}$* mice was significantly extended (Figure 4A) and weight loss was reversed as compared to oil-treated controls (Figure 4B), supporting the importance of microglia and macrophages in the arrest of pathology. In order to test for specificity of Mecp2 expression after tamoxifen treatment, we placed *Cx3cr1$^{creER/+}$Mecp2$^{Lox\text{-}stop/y}$* mice on a tamoxifen diet for 3 months to maximize expression in any cells that would have the potential to recombine. As expected, we found no significant expression of Mecp2 in T or B cells, and partial re-expression in monocytes (Figure 4C), as previously reported (Yona et al., 2013). In spleen, we found a small percentage of Mecp2-expressing red pulp macrophages (~20%) (Figure 4D), consistent with the fact that red pulp macrophages do not express high amounts of CX3CR1. However, $CD64^{+}F4/80^{+}$ intestinal macrophages and microglia, in which CX3CR1 is highly expressed, had nearly 100% Mecp2 recombination (Figure 4E and 4F). Non-microglia cells in the CNS displayed no Mecp2 recombination (Figure 4G). Together, these results support that Mecp2-deficiency in microglia/macrophages contributes to pathology, and that restoring Mecp2-mediated regulation of transcriptional responses has the potential to mediate benefits in the context of whole-body Mecp2-deficiency.

Mecp2 regulates glucocorticoid and hypoxia responses in microglia and peritoneal macrophages

In order to define the functional role of Mecp2 in macrophages we examined the global gene expression profile in microglia and peritoneal macrophages derived from Mecp2-null mice. We detected increased expression of glucocorticoid induced transcriptional signature genes in Mecp2-null cells when compared to their wild type counterparts, suggesting that Mecp2 functions as a repressor of this pathway (Figure 5A–D and Tables S1-S3). Among the dysregulated genes in Mecp2-null microglia and peritoneal macrophages, *Fkbp5*, a canonical glucocorticoid target gene, was strongly upregulated (Figure 5A and 5C). A number of studies have demonstrated that Mecp2 directly represses the *Fkbp5* gene (Nuber et al., 2005; Urdinguio et al., 2008). Using chromatin immunoprecipitation analysis we demonstrated Mecp2 binding to the *Fkbp5* gene promoter in bone marrow-derived macrophages (BMDM) (Figure 5E). Furthermore, *Mecp2* deletion resulted in increased amounts of histone H4 acetylation at cis-regulatory regions of *Fkbp5* gene under basal conditions (Figure 5F). These results suggest that Mecp2 restrains *Fkbp5* gene expression through epigenetic mechanisms. ChIP analysis demonstrated the binding of nuclear receptor co-repressor 2 (Ncor2) and histone deacetylase 3 (Hdac3) to the promoter region at the *Fkbp5* gene (Figure S3). These results are consistent with the well-established role of Mecp2 in the recruitment of the Ncor2 and Hdac3 complex to target genes (Ebert et al., 2013; Lyst et al., 2013). We next examined the *Fkbp5* gene expression profile in dexamethasone-treated wild type and Mecp2-null macrophages. Our results revealed that Mecp2 controls the sensitivity of the *Fkbp5* gene to glucocorticoid stimulation. Mecp2 deletion resulted in the upregulation of *Fkbp5* gene expression under dexamethasone stimulation at a low dose normally incapable of triggering *Fkbp5* gene expression (Figure 5G).

We noticed that the glucocorticoid-induced gene set contains a number of hypoxia-inducible genes (Table S3). Furthermore, our gene set enrichment analysis demonstrated significantly increased expression of a subset of hypoxia-inducible genes in Mecp2-null microglia (Figure 5H and 5I). To validate the cell-intrinsic role for Mecp2 in the negative regulation of these hypoxia-inducible genes, we cultured BMDM under either normoxia or hypoxia conditions (1% O_2) and examined their mRNA using quantitative PCR analysis. We validated increased expression of three canonical hypoxia-inducible genes, *Hif3a*, *Ddit4*, and *Cyr61* in Mecp2-null macrophages cultured under hypoxia conditions when compared to their wild type counterparts (Figure 5J), confirming a role for Mecp2 in regulation of at least a subset of hypoxia-induced gene transcripts.

Mecp2 restrains inflammatory responses in macrophages

Our RNA-Seq analysis revealed increased expression of *Tnf* induced transcriptional signature genes in Mecp2-null microglia cells when compared to their wild type counterparts (Table S2). These results indicate that Mecp2-deficiency leads to dysregulation of inflammatory responses in microglia and macrophages. To validate this finding, we examined the role of Mecp2 in the regulation of TNF-induced inflammatory responses in macrophages. We observed increased expression of *Il6, Tnf, Cxcl2, Cxcl3, and Csf3* genes in TNF-stimulated Mecp2-null BMDM when compared to wild type counterparts (Figure 6A). In order to corroborate these findings *in vivo*, we examined the inflammatory response of

resident peritoneal macrophages. Mice were injected intraperitoneally with TNF, allowed to respond for 6 hours, and then peritoneal cells were collected by lavage. Cells from peritoneal lavage were positively selected for F4/80$^+$ macrophages via AutoMACS. Peritoneal macrophages from Mecp2-null mice injected with TNF displayed an altered transcriptional response as compared to wild type (Figure 6B), including both over- and under-expression of multiple TNF response genes. No differences in baseline expression were evident in peritoneal macrophages from mice after saline treatment (Figure S4). Targets observed *in vitro* with TNF stimulated BMDM were also over expressed in peritoneal macrophages stimulated with TNF *in vivo*, suggesting that Mecp2 has consistent transcriptional roles across macrophage populations (Figure 6A and 6B).

Csf3, the gene encoding granulocyte-colony stimulating factor (GCSF), was over expressed in TNF-stimulated Mecp2-null macrophages both *in vitro* and *in vivo* (Figure 6A and 6B). Late-phenotypic Mecp2-null mice without any manipulation also displayed increased GCSF protein in serum (Figure 6C). Since a well-established effect of GCSF is to stimulate neutrophil production (Bendall and Bradstock, 2014), we examined neutrophil numbers in Mecp2-null mice. Indeed, we found that Mecp2-null mice develop severe neutrophilia (Figure S5A and S5B). In addition, GCSF is known to drive the egress of hematopoietic stem cells (HSC) from the bone marrow (Bendall and Bradstock, 2014) and as expected, late-phenotypic Mecp2-null mice also became progressively deficient in bone marrow HSC with disease progression (Figure S5C and S5D). In order to test whether or not neutrophilia and HSC loss play a role in the disease, we treated Mecp2-null mice with a neutralizing anti-GCSF antibody beginning at age 6–7 weeks (a mid-phenotypic time-point). Flow cytometric analysis revealed rescue of neutrophilia (Figure 6D) and prevention of HSC loss (Figure S5E). The treatment also moderately increased the lifespan of Mecp2-null mice (Figure 6E).

Together, these findings implicate Mecp2 in control of the macrophage inflammatory response, which may have downstream implications for complex disease processes in the context of Mecp2-deficiency.

Discussion

In this work we have demonstrated that Mecp2 is widely expressed across macrophage populations, and that Mecp2-deficiency leads to transcriptional impairment and/or loss of macrophages in multiple tissues. Postnatal genetic rescue of several tissue- resident macrophage and monocyte populations via *Cx3cr1*^{creER} mediated expression of Mecp2 resulted in increased lifespan. We have further provided evidence that Mecp2 is required for macrophage responses to multiple stimuli through both RNA-Seq of acutely isolated Mecp2-null microglia and peritoneal macrophages, and both *in vitro* and *in vivo* validation of pathways identified through RNA-Seq. Together, these findings implicate macrophages, and potentially monocytes, as previously unrecognized players in Rett syndrome pathology. Our results also suggest that Mecp2 is an important regulator of macrophage response to stimuli/stressors, and future work examining the mechanisms of transcriptional and epigenetic regulation of macrophage responses should take into account the role of Mecp2 in macrophage activation.

These findings support the notion that both malfunction and loss of macrophages and resident monocytes may be a contributing factor in Rett syndrome pathologies occurring across multiple organ systems. Our finding that Mecp2-null macrophages display impaired response to multiple stimuli–including glucocorticoids, hypoxia, and inflammation–may be of particular importance in the context of Mecp2-deficient animals, as the level of general organ dysfunction is high compared to wild type mice; therefore, ongoing dysfunction of other cell types, such as neurons, may increase the cellular stress/activation upon Mecp2-null microglia and macrophages and thereby exacerbate their loss and/or further pathology induced by maladaptive responses to stimuli by Mecp2-null macrophages. Such a positive feedback loop involving multiple cell types and tissues could help explain the progressive development of symptoms in Mecp2-null mice, which ultimately lead to death. These results may also explain why cell-specific deletion of Mecp2 in microglia cells did not result in significant symptoms of Rett syndrome (unpublished observations); Mecp2-null microglia and macrophages represent amplifiers of pathology, driven primarily by neurons, and thus their replacement by wild type cells abrogates the otherwise vicious cycle and slows down the disease progression; however without the pathology driven by neurons (such as apneas, abnormal glucocorticoid response, etc.), Mecp2-null microglia cannot induce a Rett-like pathology.

It is well-recognized that girls suffering from Rett syndrome experience severe problems outside the CNS, such as gastrointestinal distention, defects of nutrient absorption, scoliosis, osteopenia, and general somatic growth deficits (Chahrour and Zoghbi, 2007; Dunn and MacLeod, 2001). Intestines contain a large number of immune cells, including a significant fraction of macrophages (Zigmond and Jung, 2013). Osteoclasts are key players in bone turnover and homeostasis (Davies et al., 2013). Thus, it is conceivable that pathology in both the gastrointestinal tract and the bones could be exacerbated by defects of tissue-resident macrophage function and/or loss of tissue-resident macrophages in these tissues. It has been suggested that macrophages may be one of the two largest sources of insulin-like growth factor 1 (IGF-1), which is a critical growth factor involved in growth and health of a multitude of tissues (Gow et al., 2010). In addition, IGF-1 treatment has been shown to increase the lifespan of Mecp2-null mice (Tropea et al., 2009) and recently initiated clinical trials are promising (Khwaja et al., 2014). It is therefore possible that functional defects and loss of tissue-resident macrophages in Mecp2-deficient mice, and possibly Rett syndrome, may contribute to overall pathology via deficiency of macrophage-derived IGF-1. Moreover, our RNA-seq data shows that Mecp2-null microglia express increased amounts of *Igfbp3*, a binding protein for IGF-1, which binds soluble IGF-1 and neutralizes its function.

In recent groundbreaking work examining deletion of *Mecp2* in adult mice, phenotypic progression is similar in time-scale to that seen in mice null from birth (McGraw et al., 2011). This may support the hypothesis that accumulation of cellular stress in the absence of Mecp2 is progressively detrimental to cells necessary for tissue homeostasis, such as tissue-resident macrophages.

Beyond Rett syndrome, this work suggests that Mecp2 is an epigenetic regulator of macrophages. Given the diversity and plasticity of macrophages across organ systems, understanding the role of Mecp2 in each specific macrophage population may prove a

difficult task. However, understanding the role of Mecp2 in macrophages, and the immune system as a whole, could lead to greater understanding of several diseases in addition to Rett syndrome, including MeCP2 duplication/triplication syndrome (Chahrour and Zoghbi, 2007), and systemic lupus erythematosus (Koelsch et al., 2013), which has been linked to abnormalities of MeCP2 in humans.

We found genetic dysregulation in response to multiple stimulations in Mecp2-null macrophages, which *in vivo* may act alone or in concert depending upon the exact conditions presented to the cell. For instance, many of the hypoxia-induced transcripts measured to be abnormal in Mecp2-null macrophages, were also found in the disrupted glucocorticoid pathways identified by RNA-Seq. Therefore, such transcripts might represent independent dysfunction in Mecp2-null macrophages in the context of hypoxia alone, or an additional complication of glucocorticoid-induced transcription depending on context. Further, the combination of glucocorticoid stimulation and hypoxia might result in complex transcriptional dysregulation.

Our validation studies of inflammatory-, hypoxia-, and glucocorticoid- signaling confirm a macrophage-intrinsic role for Mecp2 in proper execution of these transcriptional responses. We validated *in vitro* that stimulation of Mecp2-null macrophages demonstrates excessive and dysregulated inflammatory response and excessive response to low-dose glucocorticoids, which have been previously shown to contribute to pathology in mouse models of Mecp2-deficiency (Braun et al., 2012). Of particular note, we found that Mecp2-null mice develop an inflammatory activation of microglia with disease progression, and that resident peritoneal macrophages stimulated with TNF *in vivo*, or BMDM stimulated with TNF *in vitro*, have an abnormal transcriptional response which implicates Mecp2 as a key regulator of inflammatory gene programs in macrophages. Of note, TNF is a widely used cytokine with important functions in both the CNS and PNS in the context of normal, non-inflammatory function and development (Stellwagen and Malenka, 2006; Wheeler et al., 2014). Based on what we have demonstrated in macrophages, it is possible that TNF signaling in neurons is also impaired in the absence of Mecp2, potentially contributing to abnormal neuronal function and/or development in Rett syndrome. This possible cascade will be evaluated in future studies.

These results provide evidence that Mecp2 plays an important role in the epigenetic regulation of macrophage responses and implicate macrophages as therapeutic targets in Rett syndrome. Importantly, we found that three stimuli (glucocorticoids, hypoxia, and inflammation) were transcriptionally dysfunctional in the absence of Mecp2, associating Mecp2 as a widely used epigenetic regulator in macrophages. Given that Mecp2 regulates multiple response pathways in macrophages, it is important to note that the exact effects of Mecp2-deficiency in macrophages in the context of a severe whole-body disease such as Rett syndrome becomes extremely difficult to predict, especially when one considers the variation in location, context, and functions of macrophages throughout the body. Thus, future studies should consider Mecp2 as an important player in the transcriptional regulation of macrophage responses and endeavor to understand the role of Mecp2 in the many unique macrophage populations.

Experimental Procedures

Additional experimental procedures can be found in the supplemental materials.

Animals

Male and female C57Bl/6J, B6.129P2(C)-*Mecp2*$^{tm1.1Bird}$/J, B6.129P2-*Mecp2*^{tm2Bird}/J, and B6.129P–*Cx3cr1*^{tm1Litt}/J mice were purchased from Jackson Laboratories and/or bred in house using stock obtained from Jackson Laboratories. *Cx3cr1*^{creER} mice were kindly provided by S. Jung (Weizmann Institute of Science, Rehovot, Israel) and were maintained in our laboratory on C57Bl/6J background. All animals were housed in temperature and humidity controlled rooms, and maintained on a 12 h/12 h light/dark cycle (lights on at 7:00). All strains were kept in identical housing conditions. Mice were scored for pathology based on a 3-point scale across four categories: hind-limb-clasping, tremors, gait, and general appearance. For each category, 3 = wild type, 2 = mid-phenotypic, and 1 = late-phenotypic. Mice that scored in-between 3 and 2 were considered early/pre-phenotypic. Approximate ages for pre-phenotypic mice were 4–5 weeks, and for late-phenotypic 8–12 weeks; however, all experiments were performed and labeled based on actual phenotype of the mice. All procedures complied with regulations of the Institutional Animal Care and Use Committee at The University of Virginia.

Tamoxifen treatment

Tamoxifen (Sigma T5648) was solubilized in corn oil (Sigma) at 10 mg/ml. Mice were injected 3 times, subcutaneously, between the shoulder blades, at 48 h intervals at a dose of 100 mg/kg. For tamoxifen feeding, mice were placed on tamoxifen diet TD.130856 (Harlan Laboratories) for up to 3 months before analysis, while controls were left on normal mouse chow (Harlan Laboratories).

RNA-seq analysis

Total RNA was extracted using the RNeasy mini kit (Qiagen). RNA-Seq was performed by Hudson Alpha Genomic Services Laboratory. Statistical analysis and data postprocessing were performed with in-house developed functions in Matlab (Litvak et al., 2009; Litvak et al., 2012). For transcriptome analysis of wild type and Mecp2-null microglia and peritoneal macrophages, genes were selected for inclusion on the basis of filtering for minimum log2 expression intensity (>4).

Gene Set Enrichment Analysis

GSEA is an analytical tool for relating differentially regulated genes to transcriptional signatures and molecular pathways associated with known biological functions[3]. The statistical significance of the enrichment of known transcriptional signatures in a ranked list of genes was determined as described (Subramanian et al., 2005). To assess the phenotypic association with Mecp2 deficiency, we used the list of genes that was ranked according to differential gene expression in Mecp2-null and wild type microglia. We used 4,722 gene sets from the Molecular Signature Database C2 version 4.0 and 32 custom gene sets including hypoxia and glucocorticoid-stimulated gene sets (Table S1).

Quantitative chromatin immunoprecipitation (ChIP) analysis

For ChIP analysis formalin-fixed cells were sonicated and processed for immunoprecipitation essentially as described (Ning et al., 2011). In brief, 1.5×10^7 BMMs were cross-linked for 10 min in 1% paraformaldehyde, washed and lysed. Chromatin was sheared by sonication (5 × 60 s at 30% maximum potency) to fragments of approximately 150 bp. For anti-Mecp2 antibodies ChIP, the sheared chromatin was incubated with Mecp2 (ABE171) (Millipore), and then immunoprecipitated using anti-rabbit IgG Dynabeads (Invitrogen) pre-conjugated with anti-Chicken IgY antibodies (ab6877) (Abcam); washed and eluted. For acH4 ChIP, the sheared chromatin was incubated with anti-rabbit IgG Dynabeads (Invitrogen) pre-conjugated with antibodies acH4 (06–598) (Upstate) or Isotype control IgG1 (BD Pharmigen); washed and eluted. Eluted chromatin was reverse-cross-linked, and DNA was purified using phenol/chloroform/isoamyl extraction.

For quantitative ChIP, immunoprecipitated DNA samples were amplified with *Fkbp5*-promoter-specific primers (Forward: TGCACTGCCTATGCAAATGA and Reverse: AGCTTCCTCCATCCCTCTT) using TaqMan quantitative PCR analysis. PCR samples from IgY-ChIPs served as a negative control.

Accession numbers

The Gene Expression Omnibus (GEO) accession number for the RNA-Seq data reported in this paper is GSE66211. http://www.ncbi.nlm.nih.gov/geo/query/acc.cgi?acc=GSE66211

The Gene Expression Omnibus (GEO) accession number for the ChIP-Seq data reported in this paper is GSE66502. http://www.ncbi.nlm.nih.gov/geo/query/acc.cgi?acc=GSE66502

Supplementary Material

Refer to Web version on PubMed Central for supplementary material.

Acknowledgments

We thank Shirley Smith for editorial assistance and Dr. Alex Koeppel (Bioinformatics core, School of Medicine, University of Virginia) for his initial analysis of RNA-Seq data. We thank Dr. Arthur Mercurio and Bryan Pursell (Department of Molecular, Cell and Cancer Biology, UMass Medical School) for their help with hypoxia experiments. We thank the members of the Kipnis lab as well as the members of the Center for Brain Immunology and Glia (BIG) for their valuable comments during multiple discussions of this work. Noël C. Derecki was supported by Hartwell Foundation post-doctoral fellowship. James C. Cronk was supported by an award from the National Institute of Allergy and Infectious Diseases 1F30AI109984. This work was primarily supported by a grant from the National Institutes of Neurological Disorders and Stroke NS081026 (J. K), the Simons Foundation Autism Research Initiative (J. K.), and from the Rett Syndrome Research Trust (J. K.).

References

Amir RE, Van den Veyver IB, Wan M, Tran CQ, Francke U, Zoghbi HY. Rett syndrome is caused by mutations in X-linked MECP2, encoding methyl-CpG-binding protein 2. Nature genetics. 1999; 23:185–188. [PubMed: 10508514]

Bain CC, Scott CL, Uronen-Hansson H, Gudjonsson S, Jansson O, Grip O, Guilliams M, Malissen B, Agace WW, Mowat AM. Resident and pro-inflammatory macrophages in the colon represent alternative context-dependent fates of the same Ly6Chi monocyte precursors. Mucosal immunology. 2013; 6:498–510. [PubMed: 22990622]

Ballas N, Lioy DT, Grunseich C, Mandel G. Non-cell autonomous influence of MeCP2-deficient glia on neuronal dendritic morphology. Nature neuroscience. 2009; 12:311–317.

Bendall LJ, Bradstock KF. G-CSF: From granulopoietic stimulant to bone marrow stem cell mobilizing agent. Cytokine & growth factor reviews. 2014; 25:355–367. [PubMed: 25131807]

Braun S, Kottwitz D, Nuber UA. Pharmacological interference with the glucocorticoid system influences symptoms and lifespan in a mouse model of Rett syndrome. Human molecular genetics. 2012; 21:1673–1680. [PubMed: 22186023]

Butovsky O, Jedrychowski MP, Moore CS, Cialic R, Lanser AJ, Gabriely G, Koeglsperger T, Dake B, Wu PM, Doykan CE, et al. Identification of a unique TGF-beta-dependent molecular and functional signature in microglia. Nature neuroscience. 2014; 17:131–143.

Chahrour M, Zoghbi HY. The story of Rett syndrome: from clinic to neurobiology. Neuron. 2007; 56:422–437. [PubMed: 17988628]

Dai XM, Ryan GR, Hapel AJ, Dominguez MG, Russell RG, Kapp S, Sylvestre V, Stanley ER. Targeted disruption of the mouse colony-stimulating factor 1 receptor gene results in osteopetrosis, mononuclear phagocyte deficiency, increased primitive progenitor cell frequencies, and reproductive defects. Blood. 2002; 99:111–120. [PubMed: 11756160]

Davies LC, Jenkins SJ, Allen JE, Taylor PR. Tissue-resident macrophages. Nature immunology. 2013; 14:986–995. [PubMed: 24048120]

Derecki NC, Cronk JC, Lu Z, Xu E, Abbott SB, Guyenet PG, Kipnis J. Wild-type microglia arrest pathology in a mouse model of Rett syndrome. Nature. 2012; 484:105–109. [PubMed: 22425995]

Dunn HG, MacLeod PM. Rett syndrome: review of biological abnormalities. Can J Neurol Sci. 2001; 28:16–29. [PubMed: 11252289]

Ebert DH, Gabel HW, Robinson ND, Kastan NR, Hu LS, Cohen S, Navarro AJ, Lyst MJ, Ekiert R, Bird AP, Greenberg ME. Activity-dependent phosphorylation of MeCP2 threonine 308 regulates interaction with NCoR. Nature. 2013; 499:341–345. [PubMed: 23770587]

Faustino JV, Wang X, Johnson CE, Klibanov A, Derugin N, Wendland MF, Vexler ZS. Microglial cells contribute to endogenous brain defenses after acute neonatal focal stroke. The Journal of neuroscience : the official journal of the Society for Neuroscience. 2011; 31:12992–13001. [PubMed: 21900578]

Ginhoux F, Greter M, Leboeuf M, Nandi S, See P, Gokhan S, Mehler MF, Conway SJ, Ng LG, Stanley ER, et al. Fate mapping analysis reveals that adult microglia derive from primitive macrophages. Science. 2010; 330:841–845. [PubMed: 20966214]

Goldmann T, Wieghofer P, Muller PF, Wolf Y, Varol D, Yona S, Brendecke SM, Kierdorf K, Staszewski O, Datta M, et al. A new type of microglia gene targeting shows TAK1 to be pivotal in CNS autoimmune inflammation. Nature neuroscience. 2013; 16:1618–1626.

Gow DJ, Sester DP, Hume DA. CSF-1, IGF-1, and the control of postnatal growth and development. J Leukoc Biol. 2010; 88:475–481. [PubMed: 20519640]

Guy J, Cheval H, Selfridge J, Bird A. The role of MeCP2 in the brain. Annual review of cell and developmental biology. 2011; 27:631–652.

Hashimoto D, Chow A, Noizat C, Teo P, Beasley MB, Leboeuf M, Becker CD, See P, Price J, Lucas D, et al. Tissue-resident macrophages self-maintain locally throughout adult life with minimal contribution from circulating monocytes. Immunity. 2013; 38:792–804. [PubMed: 23601688]

Jung S, Aliberti J, Graemmel P, Sunshine MJ, Kreutzberg GW, Sher A, Littman DR. Analysis of fractalkine receptor CX(3)CR1 function by targeted deletion and green fluorescent protein reporter gene insertion. Mol Cell Biol. 2000; 20:4106–4114. [PubMed: 10805752]

Khwaja OS, Ho E, Barnes KV, O'Leary HM, Pereira LM, Finkelstein Y, Nelson CA 3rd, Vogel-Farley V, DeGregorio G, Holm IA, et al. Safety, pharmacokinetics, and preliminary assessment of efficacy of mecasermin (recombinant human IGF-1) for the treatment of Rett syndrome. Proceedings of the National Academy of Sciences of the United States of America. 2014; 111:4596–4601. [PubMed: 24623853]

Kierdorf K, Erny D, Goldmann T, Sander V, Schulz C, Perdiguero EG, Wieghofer P, Heinrich A, Riemke P, Holscher C, et al. Microglia emerge from erythromyeloid precursors via Pu.1- and Irf8-dependent pathways. Nat Neurosci. 2013; 16:273–280. [PubMed: 23334579]

Koelsch KA, Webb R, Jeffries M, Dozmorov MG, Frank MB, Guthridge JM, James JA, Wren JD, Sawalha AH. Functional characterization of the MECP2/IRAK1 lupus risk haplotype in human T cells and a human MECP2 transgenic mouse. Journal of autoimmunity. 2013; 41:168–174. [PubMed: 23428850]

Kozlowski C, Weimer RM. An automated method to quantify microglia morphology and application to monitor activation state longitudinally in vivo. PloS one. 2012; 7:e31814. [PubMed: 22457705]

Lioy DT, Garg SK, Monaghan CE, Raber J, Foust KD, Kaspar BK, Hirrlinger PG, Kirchhoff F, Bissonnette JM, Ballas N, Mandel G. A role for glia in the progression of Rett's syndrome. Nature. 475:497–500. [PubMed: 21716289]

Litvak V, Ramsey SA, Rust AG, Zak DE, Kennedy KA, Lampano AE, Nykter M, Shmulevich I, Aderem A. Function of C/EBPdelta in a regulatory circuit that discriminates between transient and persistent TLR4-induced signals. Nature immunology. 2009; 10:437–443. [PubMed: 19270711]

Litvak V, Ratushny AV, Lampano AE, Schmitz F, Huang AC, Raman A, Rust AG, Bergthaler A, Aitchison JD, Aderem A. A FOXO3-IRF7 gene regulatory circuit limits inflammatory sequelae of antiviral responses. Nature. 2012; 490:421–425. [PubMed: 22982991]

Lyst MJ, Ekiert R, Ebert DH, Merusi C, Nowak J, Selfridge J, Guy J, Kastan NR, Robinson ND, de Lima Alves F, et al. Rett syndrome mutations abolish the interaction of MeCP2 with the NCoR/SMRT co-repressor. Nature neuroscience. 2013; 16:898–902.

Maezawa I, Jin LW. Rett syndrome microglia damage dendrites and synapses by the elevated release of glutamate. J Neurosci. 30:5346–5356. [PubMed: 20392956]

Maezawa I, Jin LW. Rett syndrome microglia damage dendrites and synapses by the elevated release of glutamate. The Journal of neuroscience : the official journal of the Society for Neuroscience. 2010; 30:5346–5356. [PubMed: 20392956]

McGraw CM, Samaco RC, Zoghbi HY. Adult neural function requires MeCP2. Science. 2011; 333:186. [PubMed: 21636743]

Nguyen MV, Felice CA, Du F, Covey MV, Robinson JK, Mandel G, Ballas N. Oligodendrocyte lineage cells contribute unique features to Rett syndrome neuropathology. The Journal of neuroscience : the official journal of the Society for Neuroscience. 2013; 33:18764–18774. [PubMed: 24285883]

Nicol JW, Helt GA, Blanchard SG Jr, Raja A, Loraine AE. The Integrated Genome Browser: free software for distribution and exploration of genome-scale datasets. Bioinformatics. 2009; 25:2730–2731. [PubMed: 19654113]

Ning S, Pagano JS, Barber GN. IRF7: activation, regulation, modification and function. Genes and immunity. 2011; 12:399–414. [PubMed: 21490621]

Nuber UA, Kriaucionis S, Roloff TC, Guy J, Selfridge J, Steinhoff C, Schulz R, Lipkowitz B, Ropers HH, Holmes MC, Bird A. Up-regulation of glucocorticoid-regulated genes in a mouse model of Rett syndrome. Hum Mol Genet. 2005; 14:2247–2256. [PubMed: 16002417]

Ramsey SA, Knijnenburg TA, Kennedy KA, Zak DE, Gilchrist M, Gold ES, Johnson CD, Lampano AE, Litvak V, Navarro G, et al. Genome-wide histone acetylation data improve prediction of mammalian transcription factor binding sites. Bioinformatics. 2010; 26:2071–2075. [PubMed: 20663846]

Schneider A, Kuhn HG, Schabitz WR. A role for G-CSF (granulocyte-colony stimulating factor) in the central nervous system. Cell cycle. 2005; 4:1753–1757. [PubMed: 16258290]

Schulz C, Gomez Perdiguero E, Chorro L, Szabo-Rogers H, Cagnard N, Kierdorf K, Prinz M, Wu B, Jacobsen SE, Pollard JW, et al. A lineage of myeloid cells independent of Myb and hematopoietic stem cells. Science. 2012; 336:86–90. [PubMed: 22442384]

Shahbazian MD, Antalffy B, Armstrong DL, Zoghbi HY. Insight into Rett syndrome: MeCP2 levels display tissue- and cell-specific differences and correlate with neuronal maturation. Human molecular genetics. 2002; 11:115–124. [PubMed: 11809720]

Sica A, Mantovani A. Macrophage plasticity and polarization: in vivo veritas. The Journal of clinical investigation. 2012; 122:787–795. [PubMed: 22378047]

Stellwagen D, Malenka RC. Synaptic scaling mediated by glial TNF-alpha. Nature. 2006; 440:1054–1059. [PubMed: 16547515]

Subramanian A, Tamayo P, Mootha VK, Mukherjee S, Ebert BL, Gillette MA, Paulovich A, Pomeroy SL, Golub TR, Lander ES, Mesirov JP. Gene set enrichment analysis: a knowledge-based approach for interpreting genome-wide expression profiles. Proceedings of the National Academy of Sciences of the United States of America. 2005; 102:15545–15550. [PubMed: 16199517]

Sunderkotter C, Nikolic T, Dillon MJ, Van Rooijen N, Stehling M, Drevets DA, Leenen PJ. Subpopulations of mouse blood monocytes differ in maturation stage and inflammatory response. Journal of immunology. 2004; 172:4410–4417.

Tropea D, Giacometti E, Wilson NR, Beard C, McCurry C, Fu DD, Flannery R, Jaenisch R, Sur M. Partial reversal of Rett Syndrome-like symptoms in MeCP2 mutant mice. Proceedings of the National Academy of Sciences of the United States of America. 2009; 106:2029–2034. [PubMed: 19208815]

Urdinguio RG, Lopez-Serra L, Lopez-Nieva P, Alaminos M, Diaz-Uriarte R, Fernandez AF, Esteller M. Mecp2-null mice provide new neuronal targets for Rett syndrome. PloS one. 2008; 3:e3669. [PubMed: 18989361]

Varol C, Vallon-Eberhard A, Elinav E, Aychek T, Shapira Y, Luche H, Fehling HJ, Hardt WD, Shakhar G, Jung S. Intestinal lamina propria dendritic cell subsets have different origin and functions. Immunity. 2009; 31:502–512. [PubMed: 19733097]

Wheeler MA, Heffner DL, Kim S, Espy SM, Spano AJ, Cleland CL, Deppmann CD. TNF-alpha/TNFR1 signaling is required for the development and function of primary nociceptors. Neuron. 2014; 82:587–602. [PubMed: 24811380]

Yasui DH, Xu H, Dunaway KW, Lasalle JM, Jin LW, Maezawa I. MeCP2 modulates gene expression pathways in astrocytes. Mol Autism. 2013; 4:3. [PubMed: 23351786]

Yona S, Kim KW, Wolf Y, Mildner A, Varol D, Breker M, Strauss-Ayali D, Viukov S, Guilliams M, Misharin A, et al. Fate mapping reveals origins and dynamics of monocytes and tissue macrophages under homeostasis. Immunity. 2013; 38:79–91. [PubMed: 23273845]

Zigmond E, Jung S. Intestinal macrophages: well educated exceptions from the rule. Trends Immunol. 2013; 34:162–168. [PubMed: 23477922]

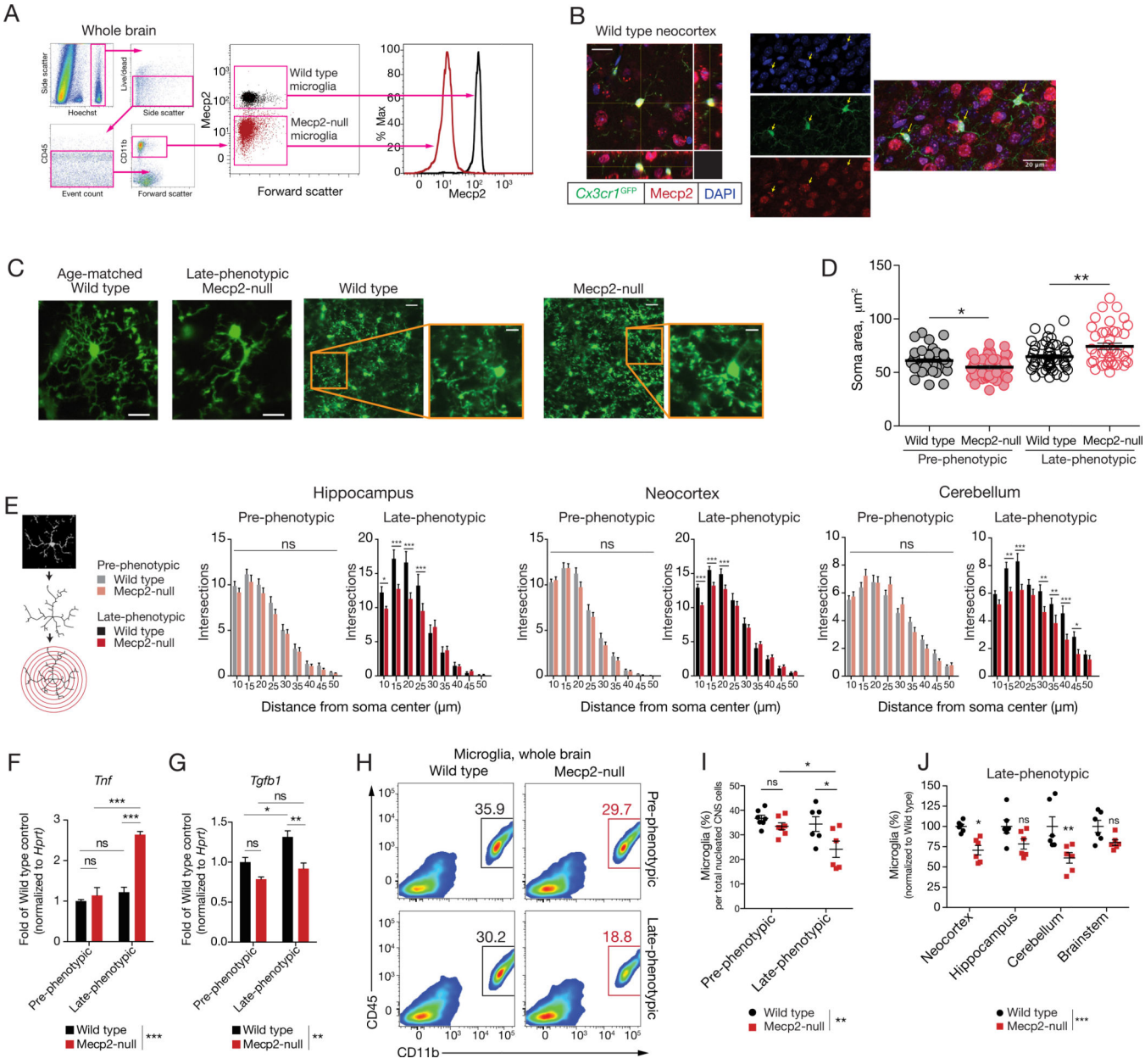

Figure 1. Microglia become activated and subsequently depleted with disease progression in Mecp2-null mice

(A) Flow cytometry demonstrating Mecp2 expression in microglia from whole brain.

(B) Cryosections from *Cx3cr1*$^{GFP/+}$ wild type mice demonstrating Mecp2 expression in microglia (scale bar, 20 µm). Images were cropped from larger images to allow for better visualization of Mecp2 localization within microglia.

(C) Representative stills from 2-photon live-imaging of late-phenotypic *Cx3cr1*$^{GFP/+}$ wild type and *Cx3cr1*$^{GFP/+}$ Mecp2-null microglia.

(D) Quantitative assessment of microglial soma size measured by two-photon intravital microscopy in pre- and late-phenotypic *Cx3cr1*$^{GFP/+}$ wild type and *Cx3cr1*$^{GFP/+}$ Mecp2-

null mice (*, $p < 0.05$; **, $p < 0.01$; two-way ANOVA with Bonferroni post-test; n = 3 mice per group. Error bars represent SEM).

(E) Sholl profiles for pre- and late-phenotypic wild type and Mecp2-null microglia in hippocampus and neocortex showing intersections; (***, $p<0.001$; **, $p<0.01$; *, $p<0.05$; two-way ANOVA with Bonferroni post-test, n = 3 mice per group with 3 separate areas from slices from identical brain structures analyzed per each genotype. Data are presented as mean ±SEM).

(F,G) qRT-PCR of *Tnf* (F) and *Tgfb1* (G) from pre- and late-phenotypic Mecp2-null mice and their age-matched wild type controls (*, $p < 0.05$; **, $p < 0.01$; two-way ANOVA with Bonferroni post-test, n = 3 mice for all groups except late-phenotypic wild type for which n = 5. Data are presented as mean ± SEM).

(H) Flow cytometric analysis demonstrating the percentage of microglia in whole brain preparations in Mecp2-null mice with increasing disease severity. Numbers show the percentage of Hoechst+ (nucleated) singlet CNS cells that are $CD45^{lo}CD11b^{+}$ microglia.

(I) Quantification of microglia in pre- and late- phenotypic Mecp2-null mice as compared to age-matched wild type controls. Cells were gated on $Hoechst^{+}$ (nucleated cells), Singlets, Size, and $CD45^{lo/neg}$ to exclude peripheral immune cells. (Two-way ANOVA with Bonferroni post-test; pre-phenotypic, not significant. Late-phenotypic; *, $p<0.05$. Pre-phenotypic vs. late-phenotypic Mecp2-null; *, $p < 0.05$. Overall main effect wild type vs. Mecp2-null; **, $p < 0.01$. n = 7 pairs of wild type and Mecp2-null mice pooled from 3 independent experiments for pre-phenotypic groups and n = 6 pairs of wild type and Mecp2-null mice pooled from 4 independent experiments for late-phenotypic groups. Error bars represent SEM).

(J) Brain region-specific microglia percentages as measured by flow cytometry in late-phenotypic Mecp2-null mice and age-matched wild type controls (*, $p < 0.05$; **, $p < 0.01$; ***, $p < 0.001$; two-way ANOVA; n = 6 mice per group. Error bars represent SEM).

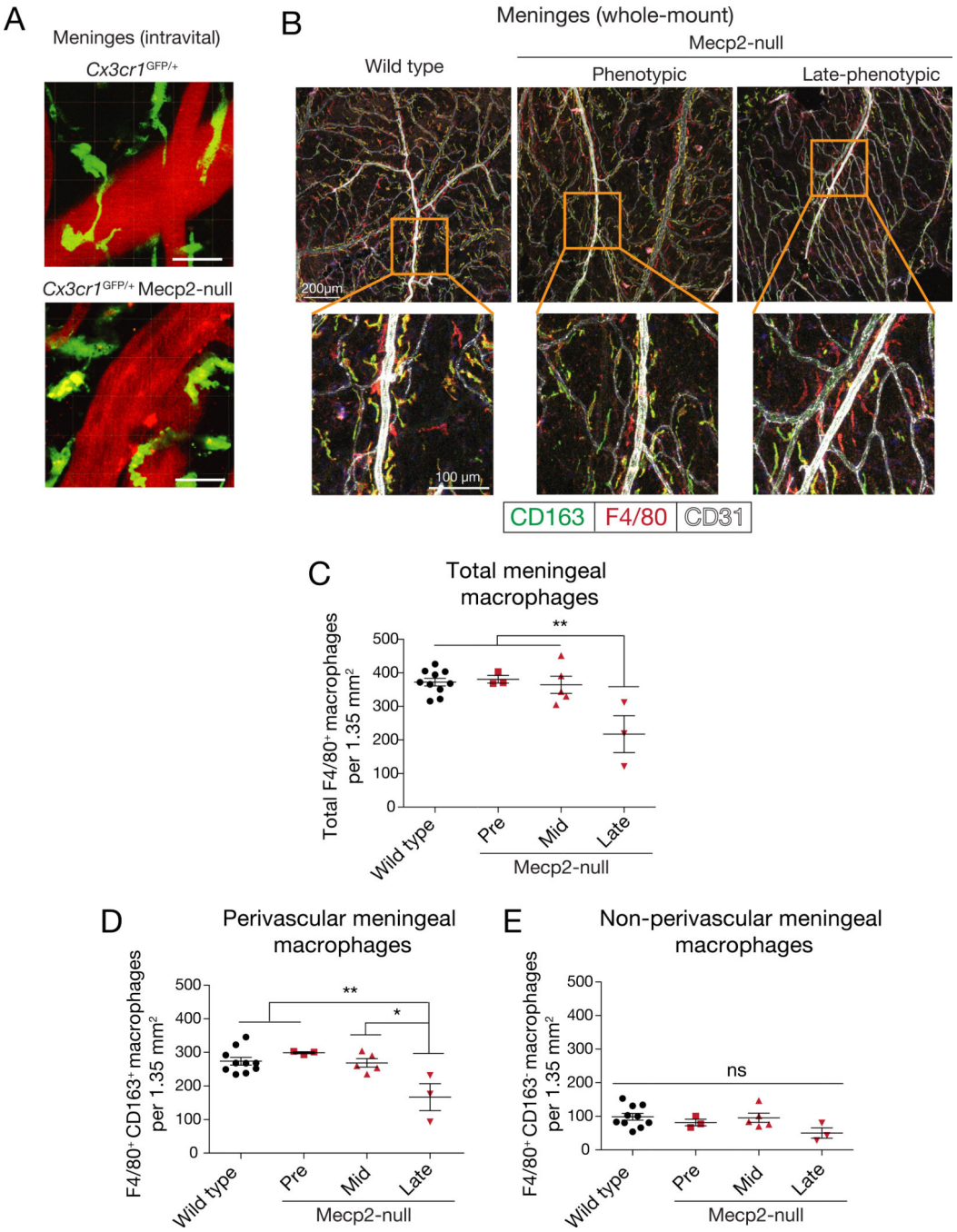

Figure 2. Meningeal macrophages are lost with disease progression in Mecp2-null mice

(A) Representative stills from intravital two-photon microscopy of phenotypic Mecp2-null meningeal macrophages demonstrating abnormal/activated morphology.

(B) Representative images of wild type, mid and late-phenotypic Mecp2-null meningeal macrophages. Upper panels, scale bar = 200μm. Lower panels, scale bar = 100μm.

(C) Quantification of total meningeal macrophages in late-phenotypic Mecp2-null mice as compared to wild type, pre- and mid-phenotypic Mecp2-null (One-way ANOVA with Bonferroni post-test; **, $p < 0.01$. Error bars represent SEM).

(D) Quantification of F4/80^{+}CD163^{+} perivascular meningeal macrophages in late-phenotypic Mecp2-null mice as compared to wild type, pre and mid-phenotypic Mecp2-null (One-way ANOVA with Bonferroni post-test; *, $p < 0.01$; **, $p < 0.01$. Error bars represent SEM).

(E) Quantification of F4/80^{+}CD163^{-}non-perivascular meningeal macrophages in Mecp2-null mice as compared to wild type (One-way ANOVA with Bonferroni post-test. Error bars represent SEM).

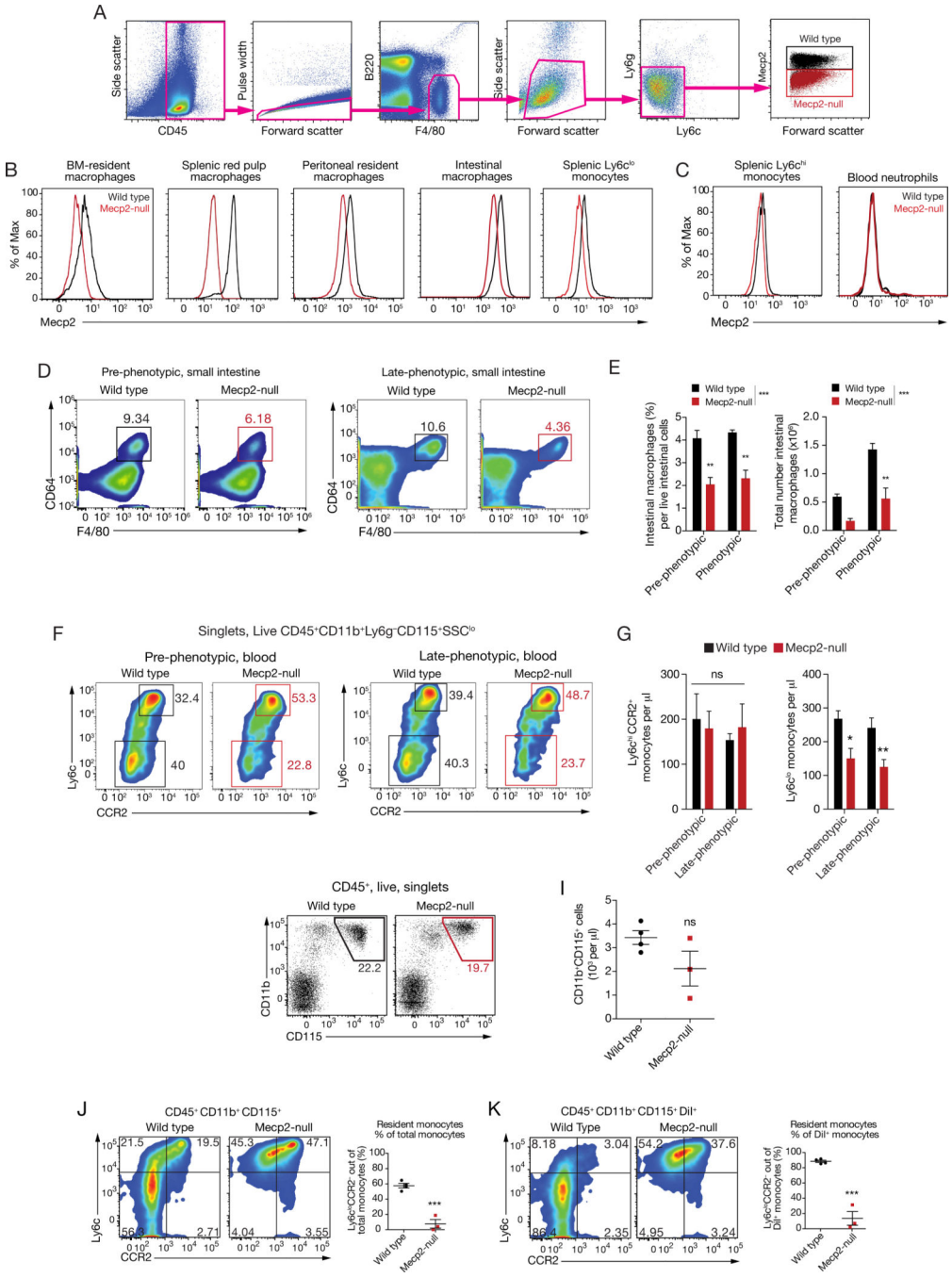

Figure 3. Peripheral monocytes and macrophages express Mecp2, and some are lost in Mecp2-null mice

(A) Example gating strategy for Mecp2 expression; shown are red pulp macrophages from spleen.

(B) Mecp2 expression in macrophage and monocyte populations as measured by intracellular flow cytometric staining in wild type and Mecp2-null mice. Gating: Bone marrow (BM)-resident macrophages-Size,CD45^{+},Singlets,Ly6c^{-},F4/80^{+},CD11b^{lo},CD3^{-} ,SSC^{lo}; Splenic red pulp macrophages-CD45^{+},Singlets,F4/80^{+},B220^{-},Size,SSC^{lo},Ly6g^{-} ,Ly6c; Peritoneal resident macrophages-

Size,Singlets,CD45$^+$,CD11b$^+$,F480^{hi}; Intestinal macrophages- Singlets,viability,CD45$^+$,CD11b$^+$,CD64$^+$; Splenic Ly6c^{lo} monocytes, CD45$^+$,Singlets, CD115$^+$,SSC^{lo},Ly6c^{lo}.

(C) Flow cytometric Mecp2 staining in inflammatory monocytes (Ly6c^{hi}CCR2$^+$) and neutrophils (Ly6g^{hi}CD11b$^+$). Gating: Splenic Ly6c^{hi}CCR2$^+$ monocytes- CD45$^+$,Singlets,CD115$^+$,SSC^{lo},Ly6c^{hi}; Neutrophils- Singlets,CD45$^+$,CD11b$^+$,Ly6g$^+$.

(D, E) Flow cytometric analysis of resident intestinal macrophages in Mecp2-null mice as compared to wild type control. (D) Representative flow cytometry plots showing the percentage of CD64$^+$F4/80$^+$ out of all CD45$^+$ intestinal cells in pre- and late-phenotypic Mecp2-null mice as compared to age-matched wild type controls. (E) Quantification of CD64$^+$CD11b$^+$ intestinal macrophages as measured by both percentage of total live intestinal cells (Two-way ANOVA with Bonferroni post-test; **, $p < 0.01$; ***, $p < 0.001$) and absolute cell counts per animal (Two-way ANOVA with Bonferroni post-test; **, $p < 0.01$; ***, $p < 0.001$). Data is representative of two independent experiments for phenotypic mice. Data are presented as mean ±SEM.

(F) Flow cytometry plots of Ly6c^{hi}CCR2$^+$ and Ly6c^{lo} blood monocytes in pre- and late-phenotypic Mecp2-null mice as compared to age-matched wild type controls. Numbers represent percentage of cells out of Singlets, Live, CD45$^+$CD11b$^+$Ly6g$^-$CD115$^+$SSC^{lo} monocytes.

(G) Quantification of numbers of circulating Ly6c^{hi}CCR2$^+$ and Ly6c^{lo} monocytes (*, $p<0.05$; **, $p<0.01$; Two-way ANOVA with Bonferroni post-test; n = 6–8 mice per group. Error bars represent SEM).

(H) Representative plots of CD11b$^+$CD115$^+$ total monocytes from blood of wild type and Mecp2-null mice on day 5 post clodronate liposome injection.

(I) Monocyte count from peripheral blood of Mecp2-null and wild type controls on day 5 post clodronate liposome injection (unpaired two-tailed Student's t-test, not significant. Error bars represent SEM).

(J) Representative flow cytometry plots displaying differentiation of Ly6c^{hi}CCR2$^+$ monocytes to Ly6c^{lo} monocytes and quantification of %Ly6c^{lo}CCR2$^-$ resident monocytes on day 5 post clodronate liposome injection; representative of two independent experiments. (***, $p<0.001$, unpaired two-tailed Student's t-test. Error bars represent SEM).

(K) Same as (J), except only DiI$^+$ monocytes are shown (cells labeled on day 2 post clodronate injection via DiI liposome injection); representative of two independent experiments. ***, $p<0.001$ (unpaired two-tailed Student's t-test. Error bars represent SEM).

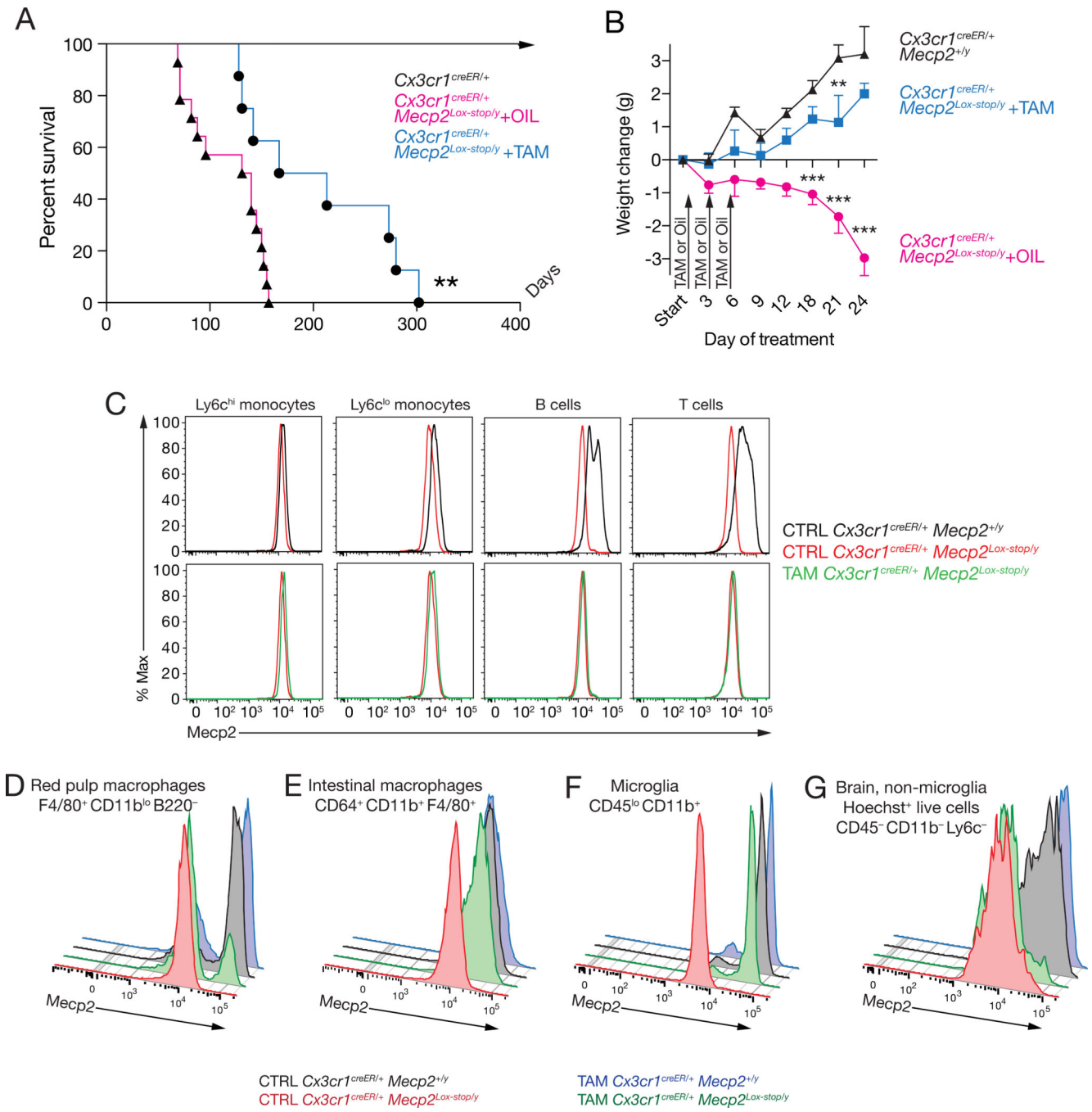

Figure 4. Postnatal expression of Mecp2 via *Cx3cr1*^{creER} in otherwise Mecp2-deficient mice increases lifespan

(A) *Cx3cr1*$^{creER/+}$*Mecp2*$^{Lox\text{-}stop/y}$ mice after postnatal tamoxifen or oil control treatment in phenotypic mice (**, p<0.01; log-rank Mantel-Cox test; tamoxifen treated n = 8, oil treated n = 12).

(B) Weight change after postnatal tamoxifen or oil control treatment in phenotypic *Cx3cr1*$^{creER/+}$*Mecp2*$^{Lox\text{-}stop/y}$ mice (**, p < 0.01; ***, p<0.001. Two-way ANOVA with Bonferroni post-test; n = 5 oil and n = 3 tamoxifen treated *Cx3cr1*$^{creER/+}$*Mecp2*$^{Lox\text{-}stop/y}$. n =

7 *Cx3cr1*$^{creER/+}$*Mecp2*$^{+/y}$ tamoxifen treated. Asterisks over *Cx3cr1*$^{creER/+}$*Mecp2*$^{Lox\text{-}stop/y}$ oil-treated indicate comparisons to *Cx3cr1*$^{creER/+}$*Mecp2*$^{Lox\text{-}stop/y}$ tamoxifen-treated. Asterisks over *Cx3cr1*$^{creER/+}$*Mecp2*$^{Lox\text{-}stop/y}$ tamoxifen-treated indicate comparisons to *Cx3cr1*$^{creER/+}$*Mecp2*$^{+/y}$. Data are presented as mean ± SEM).

(C-G) Analysis of Mecp2 re-expression in tamoxifen treated mice. Mice were fed tamoxifen food for 3 months to maximize possible recombination and analyzed by flow cytometry. Flow cytometry plots displaying Mecp2 expression in *Cx3cr1*$^{creER/+}$*Mecp2*$^{Lox\text{-}stop/y}$ mice with or without tamoxifen treatment in (C) circulating monocytes, B, and T cells; (D) red pulp macrophages; (E) intestinal macrophages; (F) microglia and (G) total non-microglia nucleated cells in the CNS.

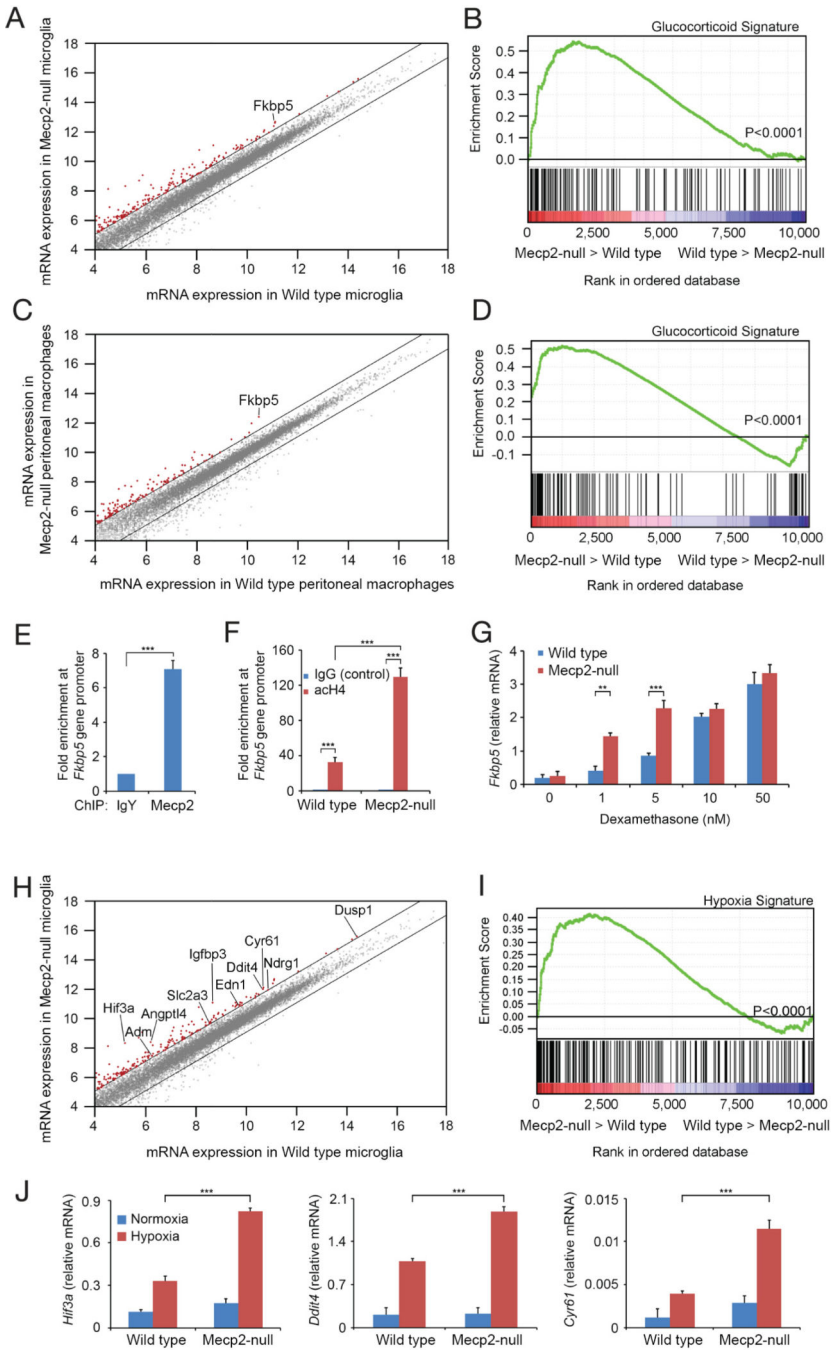

Figure 5. Mecp2 regulates glucocorticoid and hypoxia responses in microglia and peritoneal macrophages

(A) Scatter plot comparing global gene expression profiles between wild type and Mecp2-null microglia. The black lines indicate a 2-fold cut-off for the difference in gene expression levels. Data represent the average of 6 wild type and 3 Mecp2-null samples, with each sample representing 3 pooled mice (thus, 18 mice and 9 mice respectively). mRNA expression is shown on a log2 scale.

(B) Gene set enrichment analysis (GSEA) reveals the over-representation of glucocorticoid transcription signature genes in Mecp2-null microglia. The middle part of the plot shows the

distribution of the genes in the glucocorticoid transcription signature gene set ('Hits') against the ranked list of genes. Data represent the average of 6 wild type and 3 Mecp2-null samples.

(C) Scatter plot comparing global gene expression profiles between wild type and Mecp2-null peritoneal macrophages as in (A). Data represent the average of 6 pooled wild type and 6 pooled Mecp2-null mice.

(D) Global gene expression in wild type and Mecp2-null peritoneal macrophages was analyzed as in (B). Data represent the average of 6 pooled wild type and 6 pooled Mecp2-null mice.

(E) ChIP of Mecp2 from unstimulated wild type macrophages showing binding of Mecp2 to the promoter region of the *Fkbp5* gene. Data were normalized to IgY (negative control). Data represent the average of three independent experiments. *** $p < 0.001$ and ** $p < 0.01$, (unpaired two-tailed Student's t-test. Data are presented as mean ±SEM).

(F) ChIP analysis of histone H4 acetylation at the *Fkbp5* gene promoter in wild type and Mecp2-null macrophages. Data represent the average of three independent experiments (*** $p < 0.001$ and ** $p < 0.01$; unpaired two-tailed Student's t-test. Data are presented as mean ± SEM).

(G) Dexamethasone-stimulation of wild type and Mecp2-null macrophages was associated with a significant increase in *Fkbp5* mRNA levels. Dexamethasone induction of *Fkbp5* mRNA was significantly increased in Mecp2-null macrophages. Data represent the average of three independent experiments (*** $p < 0.001$ and ** $p < 0.01$; unpaired two-tailed Student's t-test. Data are presented as mean ± SEM).

(H) Scatter plot comparing global gene expression profiles between wild type and Mecp2-null microglia. The black lines indicate a 2-fold cut-off for the difference in gene expression levels. Data represent the average of 6 wild type and 3 Mecp2-null samples, with each sample representing 3 pooled mice (18 and 9 mice respectively). mRNA expression levels are on a log2 scale.

(I) Gene-set enrichment analysis (GSEA) reveals the over-representation of hypoxia signature genes in unstimulated Mecp2-null microglia.

(J) Wild type and Mecp2-null macrophages were grown in hypoxia or normoxia for 24 hrs. mRNA levels of *Hif3a Ddit4*, and *Cyr61* were measured using qRT-PCR. Results are representative of three independent experiments (average of three values ± SEM; *** $p < 0.001$ by unpaired two-tailed Student's t-test).

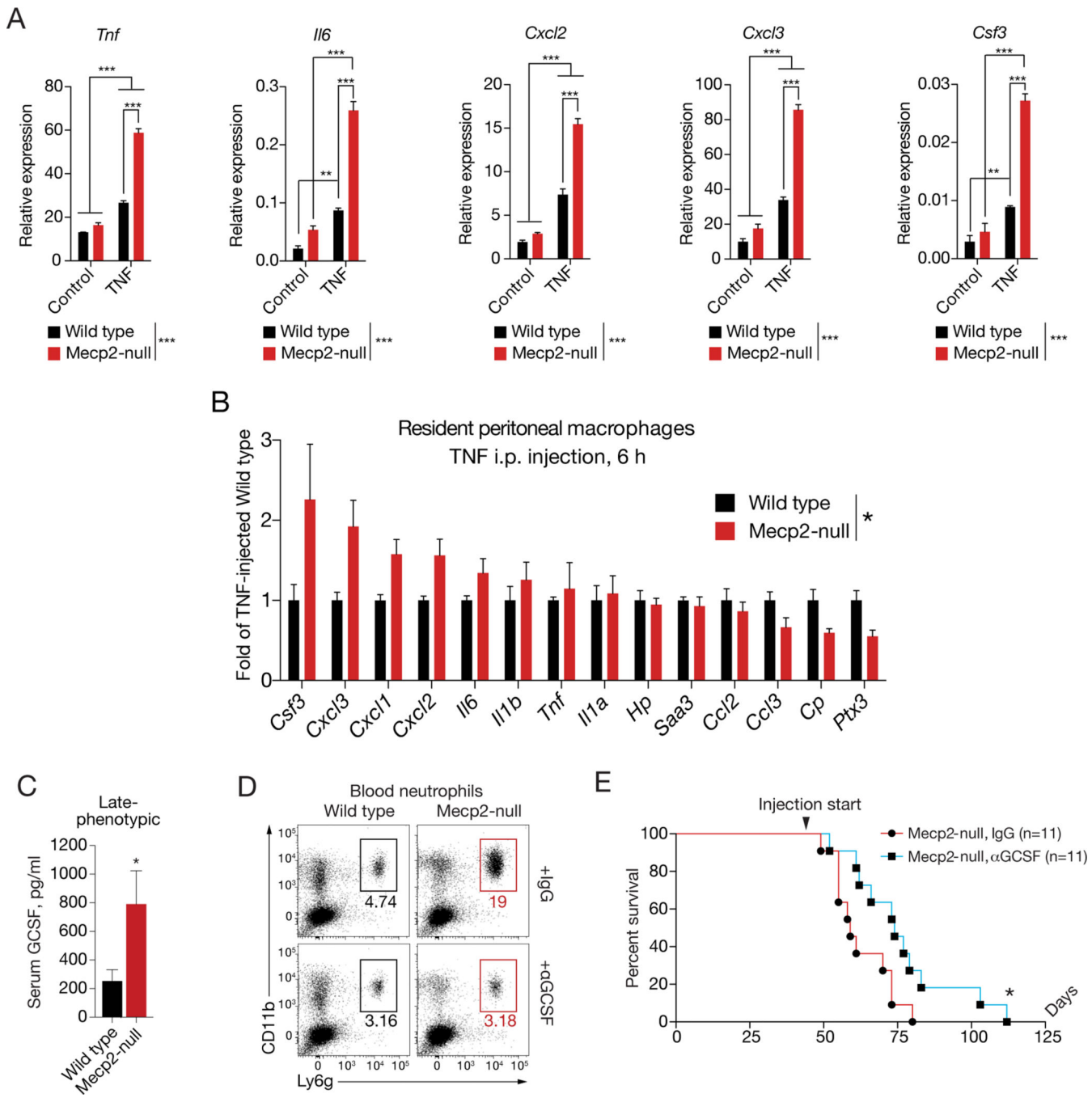

Figure 6. Mecp2 restrains inflammatory responses in macrophages

(A) Wild type and Mecp2-null macrophages were treated for 6 hr with TNF and subjected to quantitative real time PCR (qRT-PCR) for *Tnf Il6 Cxcl2 Cxcl3*, and *Csf3*. Data are representative of three experiments (average of three values ± SEM; ***, $p < 0.001$ and ** $p < 0.01$; Two-way ANOVA with Bonferroni post-test).

(B) Mecp2-null or age-matched wild type mice were injected with intraperitoneal TNF and allowed to respond for 6 hr. Resident peritoneal macrophages were collected by lavage and subsequent AutoMACS sort for F4/80$^+$ cells. RNA was collected and qRT-PCR performed

for the indicated genes (*, $p < 0.05$; Two-way ANOVA with Bonferroni post-test. Interaction for Genotype and Gene; *, $p = 0.01$. N = 3 wild type and 4 Mecp2-null. Data are presented as mean ± SEM).

(C) Granulocyte colony-stimulating factor (GCSF) ELISA of serum from late-phenotypic Mecp2-null mice and wild type controls (*, $p < 0.05$; Mann-Whitney two-tailed; n = 9 per group. Data are presented as mean ± SEM).

(D) Representative flow cytometry plots of Mecp2-null and wild type mice treated with anti-GCSF neutralizing or isotype antibodies showing percentage of neutrophils out of all $CD45^+$ circulating blood cells. Plots are representative of two independent experiments performed with n = 2 mice for all groups, analyzed 1–2 weeks post start of injections.

(E) Survival of Mecp2-null mice treated with either anti-GCSF neutralizing or isotype antibodies (*, $p < 0.05$; log-rank Mantel-Cox test; n = 11 per group).